d- or f-Mononuclear and Related Heterodinuclear Complexes With [1+1] Asymmetric Compartmental Macrocycles

Andrea Caneschi,[a] Lorenzo Sorace,[a] Umberto Casellato,[b] Patrizia Tomasin,*[b] and Pietro Alessandro Vigato[b]

Keywords: Heterometallic complexes / Macrocyclic ligands / Compartmental Schiff bases / Magnetic properties / EPR spectroscopy

d- or f-mononuclear and d,f-heterodinuclear complexes with the [1+1] asymmetric compartmental macrocycles H_2L_A, H_2L_B, H_2L_C or H_2L_D, derived from the condensation of 1,2-diaminoethane or 1,3-diaminopropane with 3,3′-(3-oxapentane-1,5-diyldioxy)bis(2-hydroxybenzaldehyde) or 3,3′-(3,6-dioxaoctane-1,8-diyldioxy)bis(2-hydroxybenzaldehyde), have been synthesized and characterized, including by single-crystal X-ray structural determinations. The influence of coordinating size and the number of donor atoms of the two adjacent chambers on the preparation of stable d,f-heterodinuclear complexes has also been tested. The X-ray structure of the isostructural complexes $[MLn(L)(Cl)_3(CH_3OH)]$ (MLn = LaCu, LaZn, TbCu) shows the metal(II) ion residing in the N_2O_2 site in a square-pyramidal coordination, the fifth apical position being filled by a chloride ion, while each lanthanide(III) ion is located in the O_2O_4 site and reaches nona-coordination by linking six oxygen atoms of the macrocyclic ligand, two chloride ions and the oxygen atom of a methanol molecule. Magnetic susceptibility data, complemented by EPR spectroscopy, of the heterodinuclear complexes, studied over the range 2–300 K, show a ferromagnetic coupling for the CuGd complex, whereas, when comparing CeCu and TbCu derivatives with the corresponding Zn derivatives, no appreciable interaction could be detected for the former and a ferromagnetic interaction seems to dominate in the latter.

Introduction

A wide range of compartmental ligands, containing adjacent similar or dissimilar coordination sites, has been designed and used in the preparation of mono- and polynuclear complexes and in studying the peculiar properties arising from the close proximity of the metal ions.[1−9]

These ligands, acyclic or cyclic, often originate from the condensation of appropriately designed formyl and amine precursors. While the acyclic ligands are always asymmetric, the cyclic ligands can be symmetric or asymmetric. X-ray structural determinations or, when lacking suitable crystals, mass spectrometry reveals conveniently their molecular complexity.[10−16] Suitable infrared and NMR investigations have added the information necessary to identify exhaustively their nature.

Asymmetric compartmental ligands have received particular attention in the last decade as they can give rise to specific molecular recognition at the two adjacent, different compartments.[17−19] Thus, they can recognize two different metal ions; the resulting heterodinuclear complexes generally show considerably different chemical and physical behaviours from those derived from the sum of the related properties of the single metal ions surrounded by the same coordination moiety.

In addition, when homodinuclear complexes are formed, the two metal ions can be varied by appropriate reactions, i.e. the selective oxidation or reduction of one metal ion, the further ligand coordination to one metal ion with the consequent variation of the coordination polyhedron, etc. These reactions, however, are difficult to fine-tune and often do not occur. Further possibilities include the migration of one metal ion from one site to the other to afford positional isomers, the substitution of one metal ion by transmetallation (inducing a consequent migration from one site to the other), and modification of the coordination environment about one metal ion through its oxidation or reduction. These molecular movements can be reversed by changing the reaction conditions or the external stimulus. Such systems are potential molecular machines, and several molecular or nanomolecular sensors or devices based on these processes have been successfully proposed.[20−22]

We have investigated recently the coordinating properties of [1+1] asymmetric cyclic Schiff bases derived from the condensation of 3,3′-(3-oxapentane-1,5-diyldioxy)bis(2-hydroxybenzaldehyde) or 3,3′-(3,6-dioxaoctane-1,8-diyl-

[a] Department of Chemistry and INSTM Research Unit, University of Florence,
Via della Lastruccia 3, 50019 Sesto Fiorentino (Fi), Italy
[b] Istituto di Chimica Inorganica e delle Superfici,
Area della Ricerca, C.so Stati Uniti 4, 35127 Padova, Italy
Fax: (internat.) + 39-049-8702911
E-mail: patrizia.tomasin@icis.cnr.it

dioxy)bis(2-hydroxybenzaldehyde) with a series of polyamines. These ligands contain an N_2O_2 or N_3O_2 Schiff base chamber and an adjacent O_2O_3 or O_2O_4 crown-ether-like chamber. They are particularly suitable for testing the chemical preference of different metal ions in coordinating one of the two adjacent coordination sites. Notably, d- or 4f-metal ions, when treated with these ligands, occupy the Schiff base or the crown-ether-like chamber, respectively, according to their "soft" or "hard" character.[23−25]

Conversely, in the presence of s-metal ions strongly coordinated in the crown-ether-like chamber, an incoming lanthanide ion is forced into the Schiff base moiety, affording well-defined heterodinuclear complexes without positional isomers, as ascertained for the complexes $[LnNa(L)(Cl)_2(CH_3OH)]$.[23] This chemical behaviour has been used successfully to design and use these systems as suitable shift reagents for the qualitative and quantitative recognition of the sodium ion. The ^{23}Na NMR resonance of the sodium cation is markedly shifted from that of the free ion by the paramagnetic Ln^{III} centre, making the heterodinuclear Ln−Na complexes very promising candidates for the development of highly effective shift reagents for metal cations of biological importance.[26−28]

Given the remarkable tendency of Schiff bases to coordinate the d-metal ions, combined with the high preference of the "hard" lanthanide(III) ions for the crown-ether site, we aimed to obtain positional pure heterodinuclear d,f complexes and studied the physicochemical properties arising from this aggregation. The two coordination chambers were progressively enlarged to find the most appropriate donor set configuration (coordination moiety) for pure, stable heterodinuclear d,f complexes.

Accordingly, the four macrocycles H_2L_A, H_2L_B,H_2Lc and H_2L_D were employed for the synthesis and physicochemical characterisation of a series of d- or f-mononuclear and d,f-heterodinuclear complexes. In particular, the X-ray single-crystal structures of some of these d,f complexes with H_2L_D and their magnetic properties were investigated in detail.

The paper aims to verify whether the reaction pathway of Scheme 1 can be followed, the difficulty encountered with the different synthetic methodologies, the best fit of the coordination chambers for the different metal ions and the physicochemical properties resulting from the close proximity of a d- and 4f-metal ion, particularly their magnetic behaviour.

Results and Discussion

Preparation of the Ligands and Related Complexes

The [1+1] asymmetric cyclic compartmental Schiff bases H_2L_A, H_2L_B, H_2L_C and H_2L_D were prepared by self-condensation of diformyl precursors 3,3′-(3-oxapentane-1,5-diyldioxy)bis(2-hydroxybenzaldehyde) or 3,3′-(3,3-dioxaoctane-1,8-diyldioxy)bis(2-hydroxybenzaldehyde)[23−25,29,31] with an equimolar amount of the appropriate diamine (1,2-diaminoethane or 1,3-diaminopropane). For the larger macrocycles H_2L_C and H_2L_D high-dilution conditions (methanol/diethyl ether, 1:200) are necessary; when high-dilution conditions are not employed, the [1+1] cyclic Schiff bases are variously contaminated by [2+2] or higher homologues.

These Schiff bases are yellow solids, stable in air, soluble in $CHCl_3$ and CH_3OH, and slightly soluble in C_2H_5OH. A

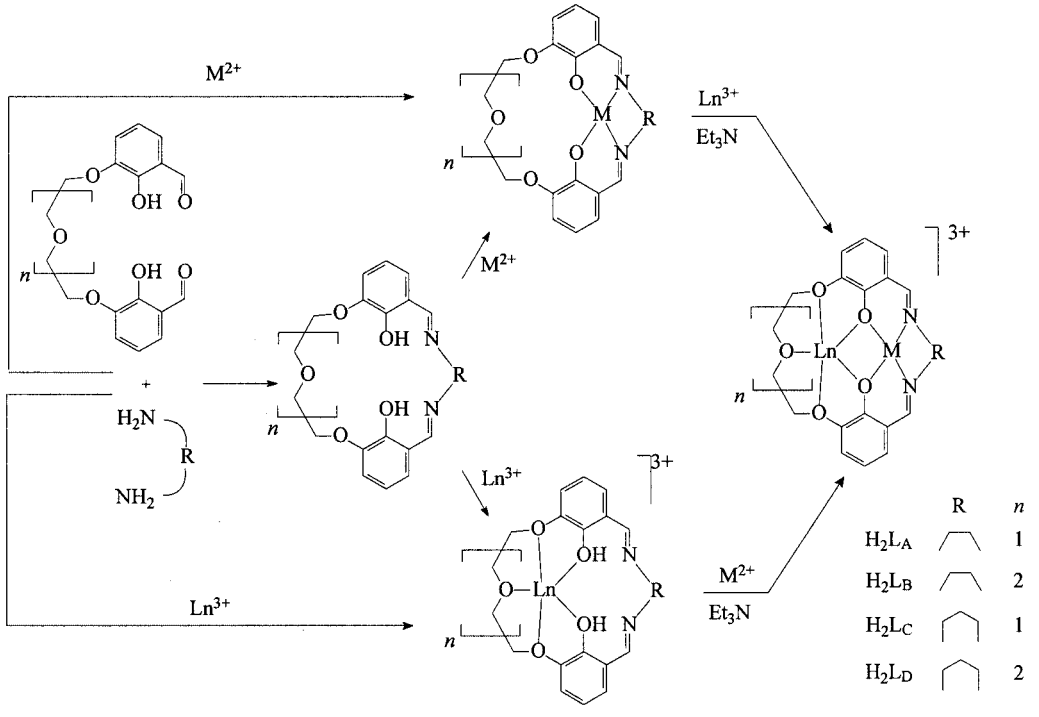

Scheme 1

strong IR band at 1635−1627 cm^{-1} due to $\nu_{C=N}$, and the absence of bands attributable to $\nu_{C=O}$ or ν_{NH2}, show that condensation occurs. ^1H NMR spectroscopy provided further evidence of condensation reactions. In particular the peaks at δ = 9.94 ppm, due to the formyl protons (CH=O), disappear and new peaks at δ = 8.30−8.19 ppm, due to the iminic protons CH=N, are clearly detectable. The other peaks, due to aliphatic or the aromatic protons, also vary because of the condensation reaction.

The [1+1] cyclic nature of $H_2L_A\cdots H_2L_D$ was inferred by FAB and ESI mass spectrometry, which clearly show two peaks at the appropriate *m*/*z* value, characteristic of the protonated $[MH]^+$ and the cationized $[MNa]^+$.

The macrocyclic Schiff bases H_2L_A, H_2L_B, H_2L_C and H_2L_D contain two adjacent coordination sites, one N_2O_2 and one O_3O_2 or O_4O_2, that are sufficiently different to give rise to two different, well-defined complexation reactions with a d- or 4f-metal ion. The N_2O_2 Schiff base site is filled exclusively by the d-metal ion while the 4f-metal ions, owing to their "harder" character, invariably coordinate the crown-like O_2O_3 or O_2O_4 chamber. The small Schiff base cavity is unsuitable for 4f-metal ion encapsulation; conversely, the "crown-ether" character of the other chamber does not favour the coordination of d-metal ions. The result is the formation of pure positional mononuclear isomers.

The appropriate diformyl derivative, 3,3′-(3,6-dioxaoctane-1,8-diyldioxy)bis(2-hydroxybenzaldehyde) or 3,3′-(3-oxapentane-1,5-diyldioxy)bis(2-hydroxybenzaldehyde), reacts in methanol in a 1:1 molar ratio with 1,2-diaminoethane or 1,3-diaminopropane in the presence of the desired transition metal(II) chloride or acetate (Cu^{2+}, Ni^{2+}, Zn^{2+}) or lanthanide(III) chloride hydrate to form the corresponding mononuclear complexes $M(L)\cdot nH_2O$ or $[Ln(H_2L)(H_2O)_4](Cl)_3$. The crude product was recrystallised from an alcoholic solution and then characterized by the usual methods.

In particular, when copper(II) salts were used, the complexes $[Cu(L)]\cdot H_2O$ were obtained, as confirmed by ESI mass spectra, which exhibits the parent peak $[Cu(L)]^+$ at the appropriate *m*/*z* value. With the other metal ions M(L), M(HL)(X) or $M(H_2L)(X)_2$ (X = Cl^- or CH_3COO) are obtained, depending on the experimental conditions. In strong basic media the complexes $M(L)\cdot nH_2O$ are obtained. These data are in line with a parallel potentiometric study showing that the different complexes $[M(H_2L)]^{2+}$, $[M(HL)]^+$ and [M(L)] are the predominant species in particular pH ranges.[32] These investigations also prove that the coordination of a metal ion (i.e. Cu^{2+}) strongly stabilises the Schiff bases over a large pH range (2−12) and prevents their easy hydrolysis. Interestingly, this result affords the possible use of these systems in solutions usually forbidden to the Schiff bases.

Although the preformed Schiff base can give rise to the same d- or f-mononuclear complexes, when treated with the appropriate metal salt the above template procedure has to be preferred owing to the tedious and time-consuming procedure for obtaining the [1+1] macrocycle with acceptable purity. Moreover, template procedures increase considerably the yield of the complexes.

The formation of the mononuclear complexes $[Ln(H_2L)(H_2O)_n](Cl)_3$ was inferred by IR spectra, where the $\nu_{C=N}$ band was observed in the range 1637−1653 cm^{-1} depending on the macrocycle and the lanthanide ion. NMR spectra in CD_3OD were useful only for diamagnetic or weakly paramagnetic compounds, showing the HC=N signal at δ = 8.87−8.74 ppm for the lanthanum complexes and at δ = 12.47−10.56 ppm for the cerium ones.

Proton migration from the phenol to the iminic group upon complexation, which has been seen in other similar compounds,[33] was not seen in these complexes − the experimental conditions (the use of methanol as deuterated solvent) probably prevented this observation. Furthermore, X-ray structures of H_2L_B and $[La(H_2L_B)(H_2O)_4](Cl)_3$ show the lanthanum(III) ion residing in the O_3O_2 chamber, in a monocapped square-antiprismatic coordination environment, but does not allow us to define whether the protons are linked to the phenolic oxygen atom or to iminic C=N groups.[31] The same structure was found for other lanthanide(III) complexes with H_2L_B.

The three pathways summarized in Scheme 1 {reaction of $M(L)\cdot nH_2O$ with $LnCl_3\cdot nH_2O$, reactions of $[Ln(H_2L)(H_2O)_n](Cl)_3$ with metal(II) chloride, one-pot reaction} give rise to the same complexes although at times with a different solvent content. However, it was verified that the complexes $[Ln(H_2L)(H_2O)_4](Cl)_3$ are the most convenient "ligand" precursors and thus all the complexes were prepared by using the second procedure. The other two procedures were successfully tested to verify their feasibility. The one-pot reaction, in particular, clearly shows that these ligands have the correct coordination moiety for simultaneous recognition of a d- and a 4f-metal ion.

However, notably, the stability, especially in solution, of the heterodinuclear complexes $[LnM(L)(Cl)_3(CH_3OH)]$ varies considerably when changing the coordination shape of the two chambers. Thus, because the complexes $[LnM(L_A)(Cl)_3(CH_3OH)]$, though formed, are not stable enough in solution and attempts to crystallise them failed, we enlarged progressively the two bites. Again, with H_2L_B and H_2L_C, the resulting heterodinuclear complexes are unstable in solution and tend to eliminate partially one of the two metal ions. With the correct coordination shape, i.e. with ligand H_2L_D, enlarging the aliphatic chain from CH_2CH_2 to $CH_2CH_2CH_2$ in the N_2O_2 chamber and changing the crown-ether chain from O_2O_3 to O_2O_4 with the addition of a $-CH_2CH_2O-$ group, the resulting complexes are very stable in solution and readily crystallised.

Heterodinuclear complexes have been synthesised by treating $Ln(H_2L)Cl_3\cdot nH_2O$ in alcoholic solution with MCl_2 (M = Cu, Ni, Zn) in the presence of Et_3N. The solution was heated slightly during stirring: a precipitate usually formed after 20−30 min. The powder, collected by filtration and washed with $MeOH/Et_2O$, was then dissolved in an alcoholic solvent. Slow diffusion of diethyl ether into the resulting alcoholic solution produced crystals of $MLn(L_D)Cl_3\cdot nCH_3OH\cdot mEtOH$ (Ln = La, Ce, Gd, Tb; *n* =

0−1; m = 0−2). The IR spectra of $MLn(L)Cl_3$ show a strong band ($\nu_{C=N}$) in the range 1618−1638 cm^{-1} (NiLn) or 1625−1647 cm^{-1} (CuLn) with a general lowering, more or less evident, compared to the $Ln(H_2L)Cl_3$ compounds owing to the coordination of the transition metal(II) ion into the Schiff base site. ^1H NMR spectroscopy was useful only for characterizing diamagnetic and some paramagnetic compounds. Interestingly, the coordination of M^{2+} provokes a large shift of the C=N band (for LnNi at δ = 19.38−19.45 ppm, for CeCu at δ = 53.61 ppm), confirming coordination in the Schiff base site. In these heterodinuclear complexes the Ni^{II} ion is in a high-spin state; therefore, the analogous Zn^{II} compounds were chosen as diamagnetic references in the magnetic studies reported below. SEM-EDS analysis were very useful in confirming the homogeneity of the complexes and the presence of the two metal ions in the correct ratio (Ln/M/Cl = 1:1:3).

In conclusion, the ligand H_2L_D is designed correctly for the formation of stable heterodinuclear LnM complexes. Thus, while mononuclear complexes can be obtained with all the macrocycles, the formation of heterodinuclear complexes, and especially their stability in solution, strongly depends on the experimental conditions and, above all, on the size of the donor chambers. By obtaining pure, stable heterodinuclear complexes we have clearly shown the need for appropriate molecular design of the coordinating systems.

Crystal Structures of the Heterodinuclear Complexes

Crystals of La−Cu, La−Zn and Tb−Cu complexes $[LnM(L_D)(Cl)_3(CH_3OH)]$ were obtained by slow diffusion of diethyl ether in methanolic solutions. All three complexes are monoclinic (space group $P2_1/n$) and isostructural, with four molecules in the unit cell (see Exp. Sect.). Figures 1 and 2 show ORTEP representations of the crystal structure and the coordination surroundings of the only La−Cu complex.

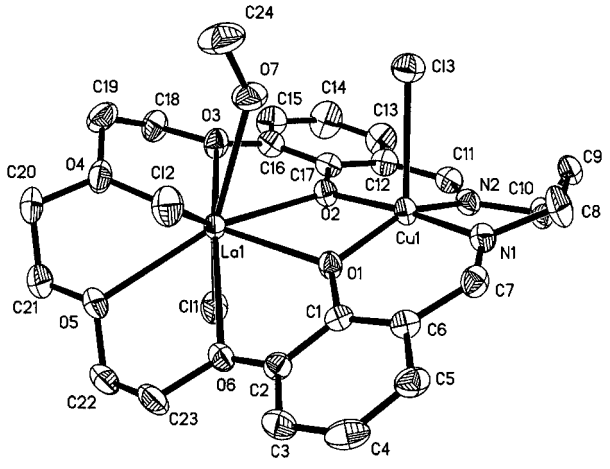

Figure 1. ORTEP diagram of the La−Cu complex showing the atom-labelling scheme; thermal ellipsoids are drawn at the 50% probability level; La−Zn and Tb−Cu complexes present an identical drawing

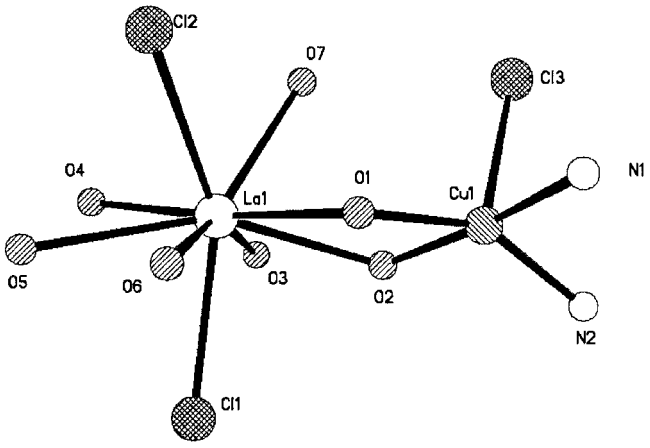

Figure 2. ORTEP diagram of the La−Cu coordination core showing the atom-labelling scheme

The macrocyclic ligand presents two coordination compartments: an N_2O_2 chamber and an O_2O_4 crown-like one. Each lanthanide metal ion is located in the O_2O_4 site and reaches the coordination number of nine by bonding six oxygen atoms of the ligand, two chlorine ions and the oxygen atom of one methanol molecule. O(3), O(4) O(5) and O(6) are etheric, whereas O(1) and O(2) are phenolic. The transition metal ions, copper and zinc, occupy the N_2O_2 chamber, the phenolic O(1) and O(2) atoms work as bridges between the coordinated metal ions.

The dimension change of the coordinated metal ions has little influence on the coordination geometry in the three complexes. Tb^{3+} (0.923Å) is smaller than La^{3+} (1.016 Å) and Cu^{2+} (0.72 Å) is smaller than Zn^{2+} (0.74 Å). Of the five possible coordination polyhedra with nine vertices, the tricapped trigonal prism and the capped square antiprism are the most stable and common in the lanthanide complexes. In our complexes, probably owing to the different nature of the coordinated oxygen atoms [etheric, phenolic and alcoholic, from O(1) to O(7)] and the presence of two chlorine ions, none of the above polyhedra can represent well the geometry around the lanthanide atoms. The best would be an hexagonal bipyramid where the base is formed by the two phenolic oxygen atoms and the four etheric oxygen atoms. One vertex is a chlorine ion, Cl(1), the other is the mid-point between the second chlorine ion, Cl(2), and the oxygen atom of the coordinated methanol molecule. The mean plane formed by the six oxygen atoms, O(1) to O(6), presents deviations in the range ±0.480 Å [the largest are +0.482 Å, for O(1), and −0.440 Å for O(4)] in both the lanthanum complexes, while the deviations are within ±0.580 Å (involving the same oxygen atoms) in the terbium complex. The lanthanide ions, in all complexes, are displaced by about 0.32 Å from the mean plane toward the Cl(2) and O(7) atoms (because of the larger hindrance of these two atoms) in relation to the only chlorine atom [Cl(1)] present in the opposite side, which forces the macrocyclic ligand to assume an umbrella-like shape. There are considerable differences in coordination bond angles on

Table 1. Metal−oxygen and metal−chlorine bonds [Å] and selected bond angles [°] in the coordination sphere of lanthanides

Donor atom	Central lanthanide ion (Ln)		
	La−Cu complex La	La−Zn complex La	Tb−Cu complex Tb
O(1)	2.460(4)	2.479(4)	2.370(8)
O(2)	2.521(4)	2.474(4)	2.447(8)
O(3)	2.710(4)	2.743(5)	2.655(8)
O(4)	2.571(5)	2.588(5)	2.480(9)
O(5)	2.662(4)	2.670(5)	2.589(10)
O(6)	2.686(4)	2.679(5)	2.650(9)
O(7)	2.566(5)	2.618(6)	2.417(11)
Cl(1)	2.804(2)	2.797(2)	2.671(4)
Cl(2)	2.818(2)	2.823(2)	2.700(3)
O(1)−Ln−O(2)	60.1(1)	61.7(1)	61.0(3)
O(1)−Ln−O(6)	60.8(1)	60.8(1)	62.2(3)
O(2)−Ln−O(3)	59.6(1)	59.1(1)	60.7(3)
O(3)−Ln−O(4)	60.6(1)	59.9(2)	61.1(3)
O(4)−Ln−O(5)	61.2(2)	60.9(2)	62.7(4)
O(5)−Ln−O(6)	60.9(1)	61.0(2)	60.4(3)
Cl(2)−Ln−O(7)	73.9(1)	73.3(1)	75.4(2)
Cl(1)−Ln−O(1)	99.3(1)	101.1(1)	101.3(2)
Cl(1)−Ln−O(2)	79.1(1)	80.1(1)	78.7(2)
Cl(1)−Ln−O(3)	74.2(1)	74.6(1)	73.3(3)
Cl(1)−Ln−O(4)	86.5(1)	85.6(2)	92.4(3)
Cl(1)−Ln−O(5)	76.0(1)	75.8(1)	74.8(3)
Cl(1)−Ln−O(6)	81.5(1)	82.3(1)	80.3(2)
Cl(1)−Ln−O(7)	138.8(1)	138.7(2)	138.5(1)
Cl(1)−Ln−Cl(2)	146.92(6)	147.22(7)	145.7(1)

changing the lanthanide ion or the transition metal ion in the complexes. Coordination bond lengths are affected by the ionic radii, which decrease on going from the lanthanum to the terbium ion and increase from the copper to the zinc ion (Tables 1 and 2).

The butterfly shape adopted by the cyclic ligand around the central ions has two phenyl rings as wings; they form a dihedral angle of between 37.3 and 38.9° in the three complexes.

The dihedral angles defined by M−O(1)−O(2) and Ln−O(1)−O(2) planes are similar in the La−Cu and Tb−Cu complexes [16.5(2) and 15.4(2)°, respectively] but is 22.9(2)° in the La−Zn complex. In the complexes, copper is more effectively replaced with zinc than lanthanum is with terbium. The polyhedron around the transition-metal ions, present in the coordination site N_2O_2, is well depicted as a square pyramid, where the base is formed by the two phenolic bridging oxygen atoms and by the two iminic nitrogen atoms, and the apex is occupied by the third chlorine ion, Cl(3). The transition-metal ion is displaced from the mean N_2O_2 plane by about 0.247 Å (mean) in the two copper-containing complexes and by 0.533 Å in the zinc complex.

The torsion angles of the ligands (O−C−C−O) and (N−C−C−C−N) are very similar (Table 3). No remarkable hydrogen-bond networks are present.

X-ray powder diffractograms of five dinuclear complexes, $CeCu(L_D)Cl_3{\cdot}CH_3OH$, $GdCu(L_D)Cl_3{\cdot}CH_3OH$, $CeZn(L_D)Cl_3{\cdot}CH_3OH$, $GdZn(L_D)Cl_3{\cdot}3H_2O$ and $TbZn(L_D)Cl_3{\cdot}EtOH$, have been compared with that obtained by calculation from single crystal diffraction data of the La−Cu complex. We conclude that Ce−Cu, Ce−Zn, Gd−Cu and La−Cu complexes are all isostructural.

Conversely, the diffractograms of Tb−Zn and Gd−Zn complexes differ from each other and from the La−Cu one. In any case, the results obtained through other physicochemical characterization techniques strongly suggest that the coordination environment of the metal ion is closely related to that observed in LaCu and isostructural compounds. This assumption, of particular importance in the following discussion on magnetic properties, is sound as the use of a compartmental ligand constrains the mutual positions of metal and bonding atoms to a fixed geometry. In this framework, the different powder diffractometric patterns observed should be ascribed more to differences in crystal packing and cell settings than to differences in coordination geometries.

Magnetic and ESR Data

The magnetic properties of coupled lanthanide ions have been the focus of intense research.[34] The main problem when dealing with these systems is the combination of the effects of the first-order angular momentum of the ground state of the lanthanide ions − with the exception of Gd^{III}− and of the crystal-field splitting, which is usually of the order of kT at room temperature. This implies that the thermal dependence of the populations of the Stark sublevels

Table 2. M−N, M−O and M−Cl bonds [Å] and selected bond angles [°] in the coordination sphere of the transition metal atoms

Donor atom	La−Cu complex Cu	La−Zn complex Zn	Tb−Cu complex Cu
O(1)	1.968(4)	2.056(4)	1.957(8)
O(2)	1.952(4)	2.065(4)	1.929(8)
N(1)	1.970(5)	2.067(6)	1.959(10)
N(2)	1.978(5)	2.058(6)	1.977(9)
Cl(3)	2.694(2)	2.347(2)	2.687(5)
Ln···M contacts	3.630(1)	3.675(1)	3.554(1)

	Dihedral angles LaCu	LaZn	TbCu
$M_4O(1)-O(2)/Ln_4O(1)-O(2)$	16.5(2)°	22.9(2)°	15.4(2)°

Central transition metal ion (M)	Cu	Zn	Cu
O(1)−M−O(2)	79.1(2)	76.1(2)	78.0(3)
O(1)−M−N(1)	92.2(2)	89.2(2)	92.6(4)
O(2)−M−N(2)	92.8(2)	88.3(2)	92.7(4)
N(1)−M−N(2)	95.5(2)	94.2(3)	96.0(4)
Cl(3)−M−O(1)	115.0(1)	120.7(1)	113.8(3)
Cl(3)−M−O(2)	86.3(1)	92.7(1)	86.9(3)
Cl(3)−M−N(1)	96.4(2)	104.6(2)	96.4(4)
Cl(3)−M−N(2)	92.4(1)	102.3(2)	92.3(4)

Table 3. Representative torsion angles [°] for the three complexes

Involved atoms	Complexes La−Cu	La−Zn	Tb−Cu
O(3)−C(18)−C(19)−O(4)	−53	−53	−51
C(19)−O(4)−C(20)−C(21)	145	145	136
O(4)−C(20)−C(21)−O(5)	55	54	49
C(20)−C(21)−O(5)−C(22)	175	176	172
O(5)−C(22)−C(23)−O(6)	−57	−57	−53
C(7)−N(1)−C(8)−C(9)	170	168	169
N(1)−C(8)−C(9)−C(10)	−46	−52	−45
C(8)−C(9)−C(10)−N(2)	82	85	82
C(9)−C(10)−N(2)−C(11)	122	126	123

has to be taken into account implicitly and an important anisotropy of the magnetic susceptibility is usually observed, preventing the use of a spin-only Hamiltonian for isotropic exchange to analyse the data. Consequently, the overwhelming majority of magnetic studies on Ln−M complexes concerns Gd^{III}-containing systems, for which the usual isotropic Heisenberg spin Hamiltonian can be employed and the interpretation of the data is straightforward.[35−40]

As a first step we determined the magnetic properties of the LaCu complex: its EPR spectrum clearly shows the features of an elongated tetragonal coordination of Cu^{II} with two broad transitions yielding $g_\perp = 2.078$ and $g_\parallel = 2.241$ (Figure 3). This is in the range usually observed for N_2O_2Cl coordination around the copper ion.[41] These results are confirmed by susceptibility measurements, which follow the Curie−Weiss law over the whole investigated temperature range (inset of Figure 3). Best-fit results to $1/\chi = (T + \theta)/C$, yielded $C = 0.422$ cm^3·K·mol^{-1} (cf. a theoretical value of 0.427 cm^3·K·mol^{-1} results from EPR) and a θ of 0.185 K, which indicates the existence of only weak antiferromagnetic intermolecular interactions.

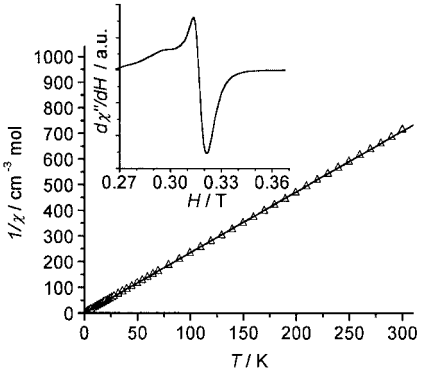

Figure 3. Curie−Weiss plot for the LaCu derivative between 2 and 300 K with the best-fit line (see text for details); inset: X-band EPR spectrum of the same complex ($g = 2.00$ is lying at $H = 0.33$ T)

The low-temperature X-band EPR spectrum of the GdZn derivative (Figure 4) exhibits fine structure due to zero-field splitting of the $S = 7/2$ state. The spectrum was satisfactorily simulated[42] by assuming a simple second-order spin Hamiltonian [$H = \beta\mathbf{B}\cdot\mathbf{g}\cdot\mathbf{S} + D\mathbf{S}_z^2 + E(\mathbf{S}_x^2-\mathbf{S}_y^2)$]

for $S = 7/2$. The best simulation was obtained using $g = 1.995 \pm .005$, $D = 0.058 \pm .002$ cm^{-1}, $E = 0.0125 \pm .001$ cm^{-1}.

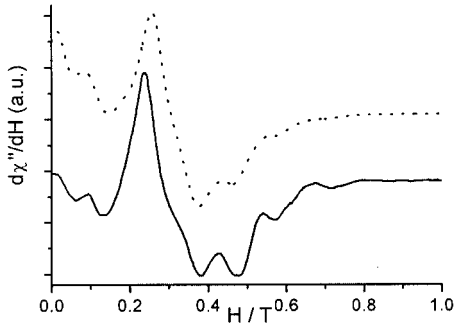

Figure 4. X-band EPR spectrum obtained for the GdZn derivative (continuous line) at 4 K, and best simulation (dotted line) obtained with parameters reported in the text; $g = 2.00$ lies at $H = 0.3300$ T

Independent determination of single-ion Cu^{II} and Gd^{III} properties was used successively to reduce the number of parameters used to fit the χT curve of GdCu (Figure 5). The χT room-temperature value obtained for this complex, 8.38 cm^3·K·mol^{-1}, is a little higher than the expected theoretical value for the two isolated $S = 1/2$ and $S = 7/2$ spins (assuming $g = 1.995$ for Gd^{III} and summing the values observed for LaCu gives 8.26 cm^3·K·mol^{-1}). On decreasing temperature, χT increases monotonically, indicating an intramolecular ferromagnetic coupling between Cu^{II} and Gd^{III} that is widely accounted for in similar systems.[35−38] The GdCu curve was then simulated by using the Hamiltonian $\mathbf{H} = J\,\mathbf{S}_{Gd}\cdot\mathbf{S}_{Cu}$ [43]

$$\chi = \frac{N\beta^2}{3kT}\cdot\frac{g_{S=4}{}^2 84 + g_{S=3}{}^2 180\exp\left(-\frac{4J}{kT}\right)}{7 + 9\exp\left(-\frac{4J}{kT}\right)}$$

where $g_{S=3} = 9/8g_{Gd} - 1/8g_{Cu}$ and $g_{S=4} = 7/8g_{Gd} + 1/8g_{Cu}$, and both g_{Cu} and g_{Gd} have been fixed to the value determined by EPR spectra of LaCu and GdZn, respectively.

Given the very small single-ion contribution to the zero-field splitting of Gd^{III} and the fairly large distance between magnetic centres of neighbouring molecules, which implies very weak intermolecular interactions, no correction[44] for these two phenomena was taken into account. The best-fit curve was obtained for $J = -2.49 \pm 0.05$ cm^{-1}, [$R^2 = \Sigma(\chi T_{calcd.} - \chi T_{obsd.})^2/\Sigma(\chi T_{obsd.})^2 = 0.9994$] meaning that the ground state $S = 4$ is separated in energy from the state $S = 3$ by about 10 cm^{-1}.

For the remaining lanthanides the situation is, as already noted, more difficult. However, some studies on the magnetic properties of anisotropic rare-earth ions coupled to either transition-metal ions or organic radicals have been reported recently.[45−50] In all these studies, the crystal-field effects on the magnetic properties of the lanthanides were determined separately by measuring a series of isomorphous complexes containing a diamagnetic counterpart (e.g. Zn^{II} or square-planar Ni^{II} in place of Cu^{II}). In the latter systems, deviation of the magnetic susceptibility compared to the Curie law is entirely due to the varying thermal population of the Ln^{III} Stark components, and this effect is assumed to be the same in systems with another paramagnetic species. In this framework, the variation with temperature of the curve obtained by subtracting the susceptibility of the complex containing the diamagnetic counterpart (e.g. LnZn) compared to that of the system with coupled centres (in our case, LnCu) ($\Delta\chi T_{LnM} = \chi T_{LnM} - \chi T_{LnZn}$) will only be due to exchange coupling interaction between the two paramagnetic centres. In detail, a positive variation of $\Delta\chi T_{LnM}$ on lowering T indicates a ferromagnetic coupling and a negative one an antiferromagnetic coupling. The same method can be applied to magnetisation measurements whenever a confirmation or a discrimination of the obtained results is needed.[47] Given the observed isostructurality of LaCu, CeCu, CeZn and TbCu, and the assumption of a closely related coordination environment for TbZn (see above), we applied this qualitative method to the family here described. Differences in crystal packing and intermolecular distances that, based on diffractometric powder pattern, might exist for TbZn are not important at this level of approximation as intermolecular interaction will not be considered.

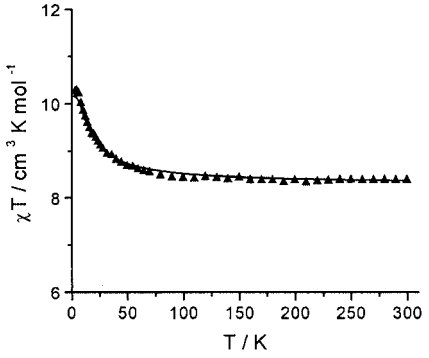

Figure 5. χT vs. T experimental curve measured between 2 and 300 K for GdCu (filled triangles), and the best-fit curve (continuous line) obtained with parameters reported in the text

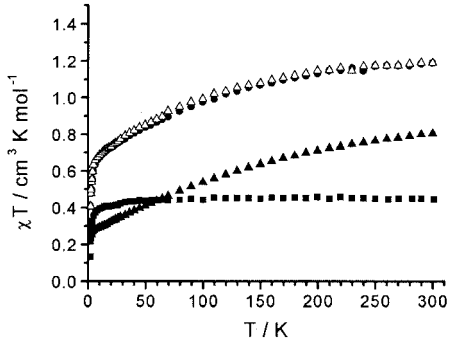

Figure 6. χT vs. T experimental curves measured between 2 and 300 K for CeCu (filled circles) and CeZn (filled triangles) and LaCu (filled squares) and the summed curve for LaCu + CeZn (open triangles)

The room-temperature value observed for the CeZn derivative, 0.80 $cm^3 \cdot K \cdot mol^{-1}$, agrees with that expected on the basis of spin-only behaviour,[51] the slow decrease observed on lowering the temperature being due to the progressive depopulation of $^2F_{5/2}$ excited Stark components (Figure 6).

Comparison of the curve resulting from the sum of LaCu and CeZn with that of CeCu clearly shows that no appreciable interaction can be observed, as the two curves are almost perfectly superimposable over the entire temperature range. Comparison of M vs. H curves measured at 2.5 K (Figure 7) might suggest the existence of a weak antiferromagnetic interaction.

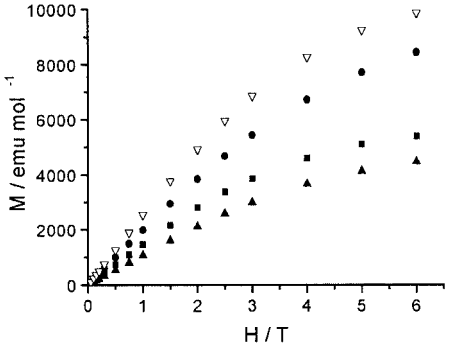

Figure 7. Comparison of the M vs. H curves at 2.5 K for CeCu (filled circles), CeZn (filled triangles), and LaCu (filled squares) with the sum (open inverted triangles) of the two latter curves

Indeed, the CeCu curve lies below the sum of LaCu and CeZn. However, in the absence of anisotropic magnetic data, diamagnetic substitution methods should not be pushed too far, and some caution should be exercised in deriving fine details.[52] In particular, some low-temperature discrepancies might well be due to small differences in crystal-field effects or intermolecular interactions and not to exchange coupling between 3d- and 4f-metal ions.

The observed χT values for the TbZn derivative at room temperature, 11.25 $cm^3 \cdot K \cdot mol^{-1}$, agrees with what is expected for this $^7F_6$ ion: on lowering the temperature the progressive depopulation of excited sublevels leads to the decrease of χT (Figure 8).

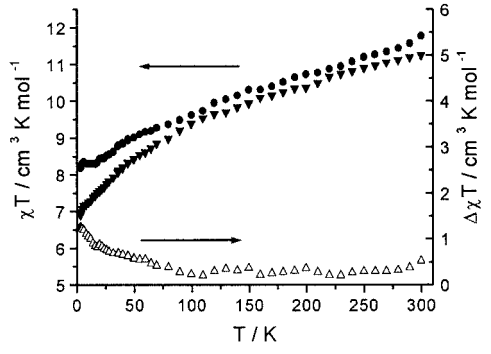

Figure 8. χT vs. T experimental curves measured between 2 and 300 K for TbCu (filled circles) and TbZn (filled inverted triangles) and their difference $\Delta\chi T$ (open triangles)

At 5 K a prominent EPR signal observed in zero field indicates that the two lowest sublevels are separated by $\Delta E = 0.3$ cm^{-1} (inset Figure 9). The results shown in Figure 8 for comparison of the χT curves of TbCu and TbZn clearly suggest a ferromagnetic coupling. Indeed, on lowering the temperature, $\Delta\chi T_{TbCu}$ increases from 0.415 $cm^3 \cdot K \cdot mol^{-1}$ at room temperature (in agreement with that observed for the LaCu derivative) to 1.25 $cm^3 \cdot K \cdot mol^{-1}$.

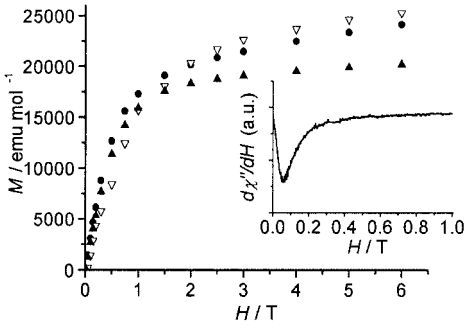

Figure 9. M vs. H curves at 2.5 K for TbCu (filled circles) and TbZn (filled triangles) compared with the sum of the latter and the experimental curve of LaCu (open inverted triangles); inset: low-temperature X-band EPR spectrum observed for the TbZn derivative

Ferromagnetic behaviour is confirmed by analysis of the M vs. H curves measured at 2.5 K (Figure 9). At low field the sum of LaCu and TbZn is lower than TbCu; however, for fields higher than 2 T the picture is reversed, which might suggest that the situation is not as simple as could be anticipated from the analysis of χT curves.

Conclusion

A series of LnM heterodinuclear complexes $[LnM(L)(Cl)_3(CH_3OH)]$ has been prepared, starting from the corresponding mononuclear complexes. It was confirmed that the transition-metal ion coordinates into the N_2O_2 Schiff base chamber while the lanthanide(III) ion prefers the O_2O_3 or O_2O_4 crown-like chamber. The two compartments of the asymmetric macrocyclic ligands have been progressively enlarged to find the best coordination moiety for heterodinuclear complexation. The larger macrocycle H_2L_D, derived from the condensation of 1,3-diaminopropane and 3,3′-(3,6-dioxaoctane-1,8-diyldioxy)bis(2-hydroxybenzoldehyde), has the most appropriate shape for forming stable heterodinuclear species. Furthermore, the large difference between two adjacent chambers assures the formation of only one species of heterodinuclear complexes, avoiding transmetallation, scrambling, migration reactions, etc. The ascertained stabilisation of the Schiff bases in consequence of the metal ion coordination opens up interesting possibilities in using these systems in solutions usually not allowed to Schiff bases.

The formation of isomerically pure, stable heterodinuclear complexes $[LnM(L_D)(Cl)_3\ (CH_3OH)]$ reported here

clearly shows the need for prior appropriate molecular design of the coordinating systems.

The prepared complexes are isostructural, with the exception of TbZn and GdZn complexes. These crystallographic differences may be ascribed more to different solvent content than to different coordination shapes about the two metal ions. Further work is in progress to clarify the origin of the crystallographic discrepancies.

As expected, we observed a ferromagnetic coupling for the GdCu complex, and the availability of a series of isomorphous LnM complexes allowed an empirical determination of the coupling interaction for two anisotropic LnCu derivatives. While no meaningful interaction was detected for the CeCu derivative, a clear sign of ferromagnetic coupling was observed for TbCu. In the absence of a simple model to explain the sign and magnitude of exchange coupling between a rare earth and an unpaired spin, we can only compare our data with the available literature results. In this respect, the observed ferromagnetic coupling for TbCu agrees with what has been found for all reported TbM couples (see ref.[49] and references cited therein), whereas a clear antiferromagnetic interaction has been reported for a different Schiff base containing CeCu complex.[45] Here, even subtle chemical and structural changes produced an observed variation of exchange coupling interaction with the Ce^{III} ion. This result points out again the need for a large wealth of data to build up a reliable magnetostrucutral correlation for complexes containing exchange-coupled lanthanide ions, in analogy to what has been done for 3d-metal ions.

Finally, functionalising these systems at the periphery of the coordination moiety with suitable hydrophilic or hydrophobic groups will increase their solubility in aqueous or non-aqueous solvents, and/or will favour their interaction and anchorage on suitable surfaces to obtain ferri- or ferromagnetic molecular nanosystems and devices. Preliminary results are very encouraging.

Experimental Section

General: All solvents, reagents and metal salts were purchased from Aldrich or Fluka and used without further purification. Dimethyl sulfoxide was purified by distillation.[53] The diformyl precursors 3,3′-(3-oxapentane-1,5-diyldioxy)bis(2-hydroxybenzaldehyde) and 3,3′-(3,6-dioxaoctane-1,8-diyldioxy)bis(2-hydroxybenzaldehyde) were prepared according to the literature.[29]

Physicochemical Characterization: Elemental analyses (C,H,N) were carried out using a Fison 1108 analyzer. IR spectra were recorded as KBr pellets with a Mattson 500 FT-IR spectrometer. ^1H and ^{13}C NMR spectra of the ligands and related complexes were performed with a Bruker AMX300 spectrometer, equipped with a 5-mm BB multinuclear probe, operating at 300.13 MHz for ^1H and 75.43 MHz for ^{13}C. 2D NOESY, 2D COSY and HMQC experiments for the ligands and complexes were performed with a Bruker AMX300 spectrometer. All the samples examined were dissolved in deuterated methanol or chloroform, which were used also as internal references. The morphology, homogeneity, and the metal/chlorine ratio of the complexes were investigated by using a Philips XL40 model scanning electron microscope equipped with an EDAXDX PRIME X-ray energy dispersive spectrometer. The solvent content (H_2O or MeOH) was evaluated by thermal analysis curves using Netzsch STA 429 thermoanalytical equipment; tests were performed under nitrogen (flux rate 250 mL/min, heating rate 5 °C min^{-1}) and in air under the same conditions. Neutral alumina (Carlo Erba, Milano, Italy) was used as reference material. ESI-MS data were recorded using a Finnigan LCQ mass spectrometer and methanolic solutions of the samples (10^{-3} M).[57] Mass spectrometric measurements were also performed using a ZAB2F instrument (Micromass, Manchester, UK) operating under FAB conditions. Nitrobenzyl alcohol solutions of the compounds were bombarded by 8 keV Xe atoms.[57] Magnetic susceptibilities of polycrystalline powders of LaCu, CeCu, CeZn, GdCu, GdZn, TbCu and TbZn were measured between 2 and 300 K with applied magnetic fields of 0.1 and 1 Tesla using a Cryogenic S600 SQUID magnetometer. To avoid the preferential orientation of polycrystalline powders, which might eventually result in a much higher apparent magnetic moment of the complexes, the powders were pressed in pellets. Data were corrected for the magnetism of the sample holder, which was determined separately in the same temperature range and field, and the underlying diamagnetism of each sample was estimated from Pascal's constants. Magnetisation measurements were performed on the same samples at 2.5 K with a field up to 6.0 T. Polycrystalline EPR powder spectra of the same complexes were recorded at the X-band (9.24 GHz) with a Varian E9 spectrometer equipped with a ^4He continuous-flow cryostat. Powders were blocked in wax to avoid preferential orientation of the crystallites.

Synthesis of Macrocycles and Complexes

H_2L_A: H_2L_A was prepared according to the literature.[31]

$Ln(H_2L_A)Cl_3{\cdot}nH_2O$ (Ln = La, Ce, Gd, Tb, Lu; n = 2−5): $LnCl_3{\cdot}6H_2O$ (2 mmol) in MeOH (5 mL) and, subsequently, ethylenediamine (120 mg, 2 mmol) in methanol (5 mL) were added to a pale yellow solution of 3,3′-(3-oxapentane-1,5-diyldioxy)bis(2-hydroxybenzaldehyde) (692 mg, 2 mmol) in methanol (50 mL). The obtained yellow solution was heated under reflux for 2.5 h and then reduced in volume. The addition of Et_2O (50 mL) to the resulting solution gave rise to a yellow precipitate that was filtered off, washed with MeOH/Et_2O (1:4), and dried in vacuo. 75% average yield.

$La(H_2L_A)Cl_3{\cdot}2H_2O$: 1004 mg, 77% yield. $C_{20}H_{22}Cl_3LaN_2O_5{\cdot}2H_2O$ (651.68): calcd. C 36.86, H 4.02, N 4.30; found C 36.14, H 3.82, N 4.27. IR: $\tilde{\nu}$ = 1648 cm^{-1} ($\nu_{C=N}$, s). ^1H NMR (300 MHz, CD_3OD, 25 °C): δ = 4.36 (m, 4 H, CH_2O), 4.39 (s, 4 H, CNCH_2), 4.45 (m, 4 H, CH_2O−Ar), 6.68 (t, 2 H, Ar−*H*), 7.15 (d, 2 H, Ar−*H*), 7.23 (d, 2 H, Ar−*H*), 8.78 (s, 2 H, *H*C=N). SEM-EDS: La/Cl = 1:3.

$Ce(H_2L_A)Cl_3{\cdot}1H_2O$: 990 mg, 78% yield. $C_{20}H_{22}CeCl_3N_2O_5{\cdot}H_2O$ (634.88): calcd. C 37.84, H 3.81, N 4.41; found C 37.62, H 3.68, N 4.54. IR: $\tilde{\nu}$ = 1649 cm^{-1} ($\nu_{C=N}$, s). ^1H NMR (300 MHz, CD_3OD, 25 °C): δ = −13.19 (d, 4 H, CH_2O), −1.19 (s, 4 H, CNCH_2), 4.20 (d, 4 H, CH_2O−Ar), 12.12 (t, 2 H, Ar−*H*), 12.47 (s, 2 H, *H*C=N), 13.05 (d, 2 H, Ar−*H*), 14.50 (d, 2 H, Ar−*H*). SEM-EDS: Ce/Cl = 1:3.

$Gd(H_2L_A)Cl_3{\cdot}2H_2O$: 994 mg, 74% yield. $C_{20}H_{22}Cl_3GdN_2O_5{\cdot}2H_2O$ (670.02): calcd. C 35.85, H 3.91, N 4.18; found C 35.16, H 4.49, N 4.63. IR: $\tilde{\nu}$ = 1637 cm^{-1} ($\nu_{C=N}$, s). SEM-EDS: Gd/Cl = 1:3.

$Tb(H_2L_A)Cl_3{\cdot}2H_2O$: 994 mg, 74% yield. $C_{20}H_{22}Cl_3N_2O_5Tb{\cdot}2H_2O$ (671.70): calcd. C 35.76, H 3.90, N 4.17; found C 35.26, H 3.72, N 4.12. IR: $\tilde{\nu}$ = 1637 cm^{-1} ($\nu_{C=N}$, s). SEM-EDS: Tb/Cl = 1:3.

Lu(H_2L_A)Cl_3·5H_2O: 1068 mg, 72% yield. $C_{20}H_{22}Cl_3LuN_2O_5$·5H_2O (741.78): calcd. C 32.38, H 4.35, N 3.78; found C 31.57, H 3.93, N 4.46. IR: $\tilde{\nu}$ = 1647cm^{-1} ($\nu_{C=N}$, s). SEM-EDS: Lu/Cl = 1:3.

Yb(H_2L_A)Cl_3·2H_2O: $YbCl_3$·6H_2O (765 mg, 2 mmol) in EtOH (20 mL) was added to a solution of H_2L_A (741 mg, 2 mmol) in chloroform (50 mL). The resulting solution was heated under reflux for 2.5 h and then reduced in volume. Addition of Et_2O (50 mL) to this solution afforded a yellow precipitate that was filtered off, washed with MeOH/Et_2O (1:4), and dried in vacuo. 878 mg, 64% yield. $C_{20}H_{22}N_2O_5YbCl_3$·2H_2O (685.81): calcd. C 35.03, H 3.82, N 4.08; found C 35.16, H 4.49, N 4.63. IR: $\tilde{\nu}$ = 1637 cm^{-1} ($\nu_{C=N}$, s). SEM-EDS: Yb/Cl = 1:3.

NiLn(L_A)Cl_3·*n*H_2O (Ln = La, Ce, Gd, Tb, Yb, Lu; *n* = 0−5): $NiCl_2$·6H_2O (237.7 mg, 1 mmol) in MeOH (5 mL) was added to a yellow solution of Ln(H_2L_A)Cl_3·*n*H_2O (1 mmol) in methanol (50 mL). After 10 min, triethylamine (202 mg, 2 mmol) was added dropwise and the resulting yellow-red solution was heated under reflux for 2.5 h. After evaporation of the solvent to dryness, the residue was treated with $CHCl_3$ (25 mL) and stirred. The orange powder obtained was filtered off, washed with Et_2O and dried in vacuo. 60% average yield.

LaNi(L_A)Cl_3·2H_2O: 452 mg, 64% yield. $C_{20}H_{20}Cl_3LaN_2NiO_5$·2$H_2O$ (708.38): calcd. C 33.07, H 3.61, N 3.86; found (%) C 33.38, H 4.46, N 3.28. IR: $\tilde{\nu}$ = 1619 cm^{-1} ($\nu_{C=N}$, s). ^{1}H NMR (300 MHz, CD_3OD, 25 °C): δ = 4.01 (s, 4 H, CH_2O), 4.77 (s, 4 H, CH_2O−Ar), 5.64 (br. s, 4 H, CNCH_2), 6.87 (t, 2 H, Ar−*H*), 7.35 (d, 2 H, Ar−*H*), 7.65 (d, 2 H, Ar−*H*), 19.38 (br. s, 2 H, *H*C=N). SEM-EDS: Ni/La/Cl = 1:1:3.

CeNi(L_A)(OH)Cl_2·H_2O: 417 mg, 62% yield. $C_{20}H_{20}CeCl_2N_2NiO_5$-(OH)·$H_2O$ (673.12): calcd. C 35.66, H 2.99, N 4.16; found C 35.33, H 3.42, N 4.22. IR: $\tilde{\nu}$ = 1618 cm^{-1} ($\nu_{C=N}$, s). ^{1}H NMR (300 MHz, CD_3OD, 25 °C): δ = −5.44 (br. s, 4 H, CH_2O), −0.24 (br. s, 4 H, CH_2O−Ar), 5.57 (d, 2 H, Ar−*H*), 6.62 (t, 2 H, Ar−*H*), 8.34 (s, 4 H, CNCH_2), 8.57 (d, 2 H, Ar−*H*), 19.45 (br. s, 2 H, *H*C=N). SEM-EDS: Ni/Ce/Cl = 1:1:2.

GdNi(L_A)Cl_3·2H_2O: 425 mg, 59% yield. $C_{20}H_{20}Cl_3GdN_2NiO_5$·2$H_2O$ (726.72): calcd. C 33.06, H 3.33, N 3.85; found C 33.69, H 4.27, N 4.46. IR: $\tilde{\nu}$ = 1634 cm^{-1} ($\nu_{C=N}$, s). SEM-EDS: Ni/Gd/Cl = 1:1:3.

TbNi(L_A)Cl_3·H_2O: 428 mg, 60% yield. $C_{20}H_{20}Cl_3N_2NiO_5Tb$·$H_2O$ (710.38): calcd. C 33.82, H 3.12, N 3.94; found (%) C 33.65, H 3.02, N 3.95. IR: $\tilde{\nu}$ = 1619 cm^{-1} ($\nu_{C=N}$, s). SEM-EDS: Ni/Tb/Cl = 1:1:3.

YbNi(L_A)$(OH)_2$Cl·5H_2O: 448 mg, 59% yield. $C_{20}H_{22}ClN_2NiO_5$-Yb$(OH)_2$·5H_2O (759.64): calcd. C 31.62, H 4.25, N 3.69; found C 30.84, H 3.70, N 4.55. IR: $\tilde{\nu}$ = 1634 cm^{-1} ($\nu_{C=N}$, s). SEM-EDS: Ni/Yb/Cl = 1:1:3.

LuNi(L_A)Cl_3·5H_2O: 460 mg, 58% yield. $C_{20}H_{20}Cl_3LuN_2NiO_5$·5$H_2O$ (798.48): calcd. C 30.09, H 3.79, N 3.51; found C 29.10, H 3.91, N 4.38 IR: $\tilde{\nu}$ = 1628 cm^{-1} ($\nu_{C=N}$, s). SEM-EDS: Ni/Lu/Cl = 1:1:3.

CuLn (L_A)Cl_3·*n*H_2O (Ln = La, Ce, Gd, Tb, Yb, Lu; *n* = 0−5): $CuCl_2$·2H_2O (170.48 mg, 1 mmol) in MeOH (5 mL) was added to a yellow solution of Ln(H_2L_A)Cl_3·*n*H_2O (1 mmol) in methanol (50 mL). After 10 min, triethylamine (202 mg, 2 mmol) was added dropwise and the resulting yellow-red solution was heated under reflux for 2.5 h. After evaporation of the solvent to dryness, the residue was treated with $CHCl_3$ (25 mL) and stirring continued. The green powder obtained was filtered off, washed with Et_2O and dried in vacuo. ca. 60% average yield.

LaCu(L_A)Cl_3·H_2O: 430 mg, 62% yield. $C_{20}H_{20}Cl_3CuN_2O_5La$·$H_2O$ (695.20): calcd. C 34.55, H 3.19, N 4.03; found C 33.73, H 3.29, N 3.42. IR: $\tilde{\nu}$ = 1645 cm^{-1} ($\nu_{C=N}$, s). SEM-EDS: Cu/La/Cl = 1:1:3.

CeCu(L_A)Cl_3·4H_2O: 484 mg, 64% yield. $C_{20}H_{20}CeCl_3CuN_2O_5$·4$H_2O$ (750.45): calcd. C 32.01, H 3.76, N 3.73; found C 31.42, H 4.12, N 3.84. IR: $\tilde{\nu}$ = 1647 cm^{-1} ($\nu_{C=N}$, s). ^{1}H NMR (300 MHz, CD_3OD, 25 °C): δ = −7.79 (s, 4 H, CH_2O−Ar), −5.44 (s, 4 H, CH_2O), −0.88 (s, 4 H, CNCH_2), 7.82 (t, 2 H, Ar−*H*), 9.49 (d, 2 H, Ar−*H*), 22.63 (d, 2 H, Ar−*H*), 53.61 (s, 2 H, *H*C=N). SEM-EDS: Cu/Ce/Cl = 1:1:3.

GdCu(L_A)Cl_3·4H_2O: 470 mg, 61% yield. $C_{20}H_{20}Cl_3CuGdN_2$-O_5·4H_2O (767.58): calcd. C 29.91, H 3.51, N 3.49; found C 29.11, H 3.98, N 4.08. IR: $\tilde{\nu}$ = 1638 cm^{-1} ($\nu_{C=N}$, s). SEM-EDS: Cu/Gd/Cl = 1:1:3.

TbCu(L_A)(OH)Cl_2·3H_2O: 442 mg, 60% yield. $C_{20}H_{20}Cl_2CuN_2O_5$-Tb(OH)·3H_2O (732.79): calcd. C 32.78, H 3.71, N 3.82; found C 32.39, H 3.10, N 3.79. IR: $\tilde{\nu}$ = 1626 cm^{-1} ($\nu_{C=N}$, s). SEM-EDS: Cu/Tb/Cl = 1:1:2.

YbCu(L_A)(OH)Cl_2·6H_2O: 456 mg, 57% yield. $C_{20}H_{20}Cl_2CuN_2O_5$-Yb(OH)·6H_2O (800.94): calcd. C 29.99, H 4.15, N 3.50; found C 29.54, H 3.40, N 4.44. IR: $\tilde{\nu}$ = 1640 cm^{-1} ($\nu_{C=N}$, s). SEM-EDS: Cu/Yb/Cl = 1:1:2.

LuCu(L_A)Cl_3·H_2O: 402 mg, 55% yield. $C_{20}H_{20}Cl_3CuLuN_2O_5$·$H_2O$ (731.26): calcd. C 32.85, H 3.03, N 3.83; found C 32.43, H 3.41, N 4.50 IR: $\tilde{\nu}$ = 1636 cm^{-1} ($\nu_{C=N}$, s). SEM-EDS: Cu/Lu/Cl = 1:1:3.

ZnLn(L_A)Cl_3·*n*H_2O (Ln = La, Ce, Tb; *n* = 0−5): $ZnCl_2$ (136.28 mg, 1 mmol) in MeOH (5 mL) was added to a yellow solution of Ln(H_2L_A)Cl_3·*n*H_2O (1 mmol) in methanol (50 mL). After 10 min, triethylamine (202 mg, 2 mmol) was added dropwise and the resulting yellow-red solution was heated under reflux for 2.5 h. After evaporation of the solvent to dryness, the resultant residue was treated with $CHCl_3$ (25 mL) and stirred. The pale yellow powder obtained was filtered off, washed with Et_2O and dried in vacuo. 60% average yield.

LaZn(L_A)Cl_3: 408 mg, 60% yield. $C_{20}H_{20}Cl_3LaN_2O_5Zn$ (679.01): calcd. C 35.38, H 2.97, N 4.13; found C 35.97, H 3.10, N 4.11. IR: $\tilde{\nu}$ = 1644 cm^{-1} ($\nu_{C=N}$, s). ^{1}H NMR (300 MHz, CD_3OD, 25 °C): δ = 3.57 (dd, 2 H, CH_2O), 3.88 (t, 2 H, CH_2O), 3.97 and 4.10 (dd, 4 H, CNCH_2), 4.31 (dd, 2 H, CH_2O), 4.88 (t, 2 H, CH_2O), 6.73 (t, 2 H, Ar−*H*), 7.18 (d, 2 H, Ar−*H*), 7.20 (d, 2 H, Ar−*H*), 8.62 (s, 2 H, *H*C=N). SEM-EDS: Zn/La/Cl = 1:1:3.

CeZn(L_A)Cl_3: 415 mg, 61% yield. $C_{20}H_{20}CeCl_3N_2O_5Zn$ (680.22): calcd. C 35.32, H 2.96, N 4.12; found C 36.08, H 3.33, N 4.17. IR data: $\tilde{\nu}$ = 1644 cm^{-1} ($\nu_{C=N}$, s). ^{1}H NMR (300 MHz, CD_3OD, 25 °C): δ = −9.88 (br. s, 2 H, CH_2O−Ar), −7.59(d, 2 H, CH_2O−Ar), −5.20 (s, 2 H, CH_2O), −3.33 (br. s, 2 H, CH_2O), 2.23 (d, 2 H, Ar−*H*), 5.48 (t, 2 H, Ar−*H*), 8.44 (s, 2 H, Ar−*H*), 8.80 (d, 2 H, CNCH_2), 9.82 (d, 2 H, CNCH_2), 12.82 (s, 2 H, *H*C=N). SEM-EDS: Zn/Ce/Cl = 1:1:3.

TbZn(L_A)Cl_3·H_2O: 422 mg, 59% yield. $C_{20}H_{20}Cl_3N_2O_5TbZn$·$H_2O$ (717.04): calcd. C 33.50, H 3.09, N 3.91; found C 33.13, H 3.34, N 3.85. IR: $\tilde{\nu}$ = 1641 cm^{-1} ($\nu_{C=N}$, s). SEM-EDS: Zn/Tb/Cl = 1:1:3.

H_2L_B: H_2L_B was prepared according to the literature.[31]

Ln(H_2L_B)Cl_3·*n*H_2O (Ln = La, Ce, Tb; *n* = 0−3): $LnCl_3$·6H_2O (2 mmol) in MeOH (5 mL) and, subsequently, ethylenediamine (120 mg, 2 mmol) in methanol (5 mL) were added to a pale yellow solution of 3,3′-(3,6-dioxaoctane-1,8-diyldioxy)bis(2-hydroxybenz-

aldehyde) (780.8 mg, 2 mmol) in methanol (50 mL). The obtained yellow solution was heated under reflux for 2.5 h and the resultant yellow precipitate was filtered off, washed with MeOH/Et_2O (1:4), and dried in vacuo. It was then recrystallised from MeOH/EtOH. 65% average yield.

$La(H_2L_B)Cl_3{\cdot}4H_2O$: 975 mg, 67% yield. $C_{22}H_{26}Cl_3LaN_2O_6{\cdot}4H_2O$ (731.76): calcd. C 36.11, H 4.68, N 3.83; found C 36.20, H 4.70, N 3.78 IR: $\tilde{\nu}$ = 1644 cm^{-1} ($\nu_{C=N}$, s). ^1H NMR (300 MHz, CD_3OD, 25 °C): δ = 4.21 (4 + 4 H, CH_2O + $CNCH_2$), 4.38 (t, 4 H, CH_2O), 4.55 (t, 4 H, CH_2O-Ar), 6.76 (t, 2 H, Ar−*H*), 7.23 (dd, 2 H, Ar−*H*), 7.37 (dd, 2 H, Ar−*H*), 8.87 (s, 2 H, *H*C=N). SEM-EDS: La/Cl = 1:3.

$Ce(H_2L_B)Cl_3$: 857 mg, 65% yield. $C_{22}H_{26}CeCl_3N_2O_6$ (660.91): calcd. C 39.98, H 3.97, N 4.24; found C 39.05, H 3.73, N 4.93. IR: $\tilde{\nu}$ = 1645 cm^{-1} ($\nu_{C=N}$, s). ^1H NMR (300 MHz, CD_3OD, 25 °C): δ = 0.14 (s, 4 H, CH_2O), 2.71 (s, 4 H, CH_2O), 4.50 (d, 2 H, Ar−*H*), 5.95 (t, 2 H, Ar−*H*), 6.24 (s, 4 H, $CNCH_2$), 7.63 (d, 2 H, Ar−*H*), 7.67 (s, 4 H, CH_2O), 10.56 (s, 2 H, *H*C=N). SEM-EDS: Ce/Cl = 1:3.

$Tb(H_2L_B)Cl_3{\cdot}3H_2O$: 931 mg, 63% yield. $C_{22}H_{26}Cl_3N_2O_6Tb{\cdot}3H_2O$ (733.76): calcd. C 36.01, H 4.40, N 3.82; found C 35.97, H 4.22, N 4.24. IR: $\tilde{\nu}$ = 1647 cm^{-1} ($\nu_{C=N}$, s). SEM-EDS: Tb/Cl = 1:3.

$NiLa(L_B)Cl_3{\cdot}nH_2O$ and $CuLa(L_B)Cl_3{\cdot}nH_2O$: These compounds were prepared according to the literature.[31]

H_2L_C: A methanolic solution (3 mL) of 1,3-diaminopropane (74 mg, 1 mmol) was diluted with diethyl ether (400 mL). A $CHCl_3$ solution (5 mL) of 3,3′-(3-oxapentane-1,5-diyldioxy)bis(2-hydroxybenzaldehyde) (346 mg, 1 mmol) was then added dropwise at room temperature. The resultant yellow precipitate was stirred for 20 min, then filtered off, washed well with a diethyl ether/light petroleum solution and dried in vacuo. 211 mg, 55% yield. $C_{21}H_{24}N_2O_5$ (384.41): calcd. C 65.62, H 6.29, N 7.29; found C 66.52, H 6.41, N 7.41. IR: $\tilde{\nu}$ = 1631 cm^{-1} ($\nu_{C=N}$, s). ^1H NMR (300 MHz, $CDCl_3$, 25 °C): δ = 2.04 (quint, 2 H, $CNCH_2CH_2$), 3.66 (t, 4 H, $CNCH_2$), 3.96 (t, 4 H, CH_2O), 4.21 (t, 4 H, CH_2O-Ar), 6.73 (t, 2 H, Ar−*H*), 6.84 (dd, 2 H, Ar−*H*), 6.94 (dd, 2 H, Ar−*H*), 8.30 (s, 2 H, *H*C=N), 13.82 (br. s, OH) ppm. MS: 385 $[M + H]^+$.

$La(H_2L_C)Cl_3{\cdot}4H_2O$: $LaCl_3{\cdot}6H_2O$ (743 mg, 2 mmol) in MeOH (5 mL) and, subsequently, 1,3-propanediamine (148 mg, 2 mmol) in methanol (5 mL) were added to a pale yellow solution of 3,3′-(3-oxapentane-1,5-diyldioxy)bis(2-hydroxybenzaldehyde) (692 mg, 2 mmol) in methanol (50 mL). The resultant yellow solution was heated under reflux for 2.5 h and then reduced in volume. The obtained yellow precipitate was filtered off, washed with MeOH/Et_2O (1:4), and dried in vacuo. 1010 mg, 72% yield. It was then recrystallised from MeOH and slow diffusion of Et_2O. $C_{21}H_{24}Cl_3LaN_2O_5{\cdot}4H_2O$ (701.74): calcd. C 35.94, H 4.60, N 3.99; found C 35.34, H 4.41, N 4.85. IR: $\tilde{\nu}$ = 1651 cm^{-1} ($\nu_{C=N}$, s). ^1H NMR (300 MHz, CD_3OD, 25 °C): δ = 2.55 (quint, 2 H, $CNCH_2CH_2$), 4.08 (t, 4 H, $CNCH_2$), 4.44 (dd, 8 H, CH_2O), 6.62 (t, 2 H, Ar−*H*), 7.00 (dd, 2 H, Ar−*H*), 7.21 (dd, 2 H, Ar−*H*), 8.74 (s, 2 H, *H*C=N). SEM-EDS: La/Cl = 1:3.

$LaNi(L_C)Cl_3$: Triethylamine (202 mg, 2 mmol) and $NiCl_2{\cdot}6H_2O$ (237.7 mg, 1 mmol), dissolved in EtOH (2 mL), were added to a yellow solution of $La(H_2L_C)Cl_3{\cdot}4H_2O$ (702 mg, 1 mmol) in ethanol (20 mL) that was slightly heated (30 °C). After stirring for 10 min, a green precipitate formed. The suspension was stirred for further 20 min and then cooled to room temperature. The resultant green powder was collected by filtration, washed with Et_2O and dried in vacuo. 357 mg, 52% yield. $C_{21}H_{22}Cl_3LaN_2NiO_5$ (686.38): calcd. C 36.75, H 3.23, N 4.08; found C 36.05, H 3.53, N 3.80 IR: $\tilde{\nu}$ = 1627 cm^{-1} ($\nu_{C=N}$, s). SEM-EDS: Ni/La/Cl = 1:1:3.

H_2L_D: A methanolic solution (3 mL) of 1,3-diaminopropane (74 mg, 1 mmol) was diluted with diethyl ether (400 mL). A $CHCl_3$ solution (5 mL) of 3,3′-(3,6-dioxaoctane-1,8-diyldioxy)bis(2-hydroxybenzaldehyde) (392 mg, 1 mmol) was then added dropwise at room temperature. The resultant yellow precipitate was stirred for 20 min, then filtered off, washed well with a diethyl ether/light petroleum solution and dried in vacuo. 300 mg, 70% yield. $C_{23}H_{28}N_2O_6$ (428.46): calcd. C 64.48, H 6.59, N 6.54; found C 64.02, H 6.42, N 6.45. IR: $\tilde{\nu}$ = 1635−1627 cm^{-1} ($\nu_{C=N}$, s). ^1H NMR (300 MHz, $CDCl_3$, 25 °C): δ = 2.03 (quint., 2 H, $CNCH_2CH_2$), 3.65 (t, 4 H, $CNCH_2$), 3.73 (s, 4 H, CH_2O), 3.88 (t, 4 H, CH_2O), 4.18 (t, 4 H, CH_2O-Ar), 6.72 (t, 2 H, Ar−*H*), 6.83 (dd, 2 H, Ar−*H*), 6.93 (dd, 2 H, Ar−*H*), 8.29 (s, 2 H, *H*C=N), 13.83 (br. s, OH) ppm. MS: 429 $[M + H]^+$.

$Ln(H_2L_D)Cl_3{\cdot}nH_2O$ (Ln = La, Ce, Gd, Tb; n = 0−7): $LnCl_3{\cdot}nH_2O$ (2 mmol) in MeOH (5 mL) and, subsequently, 1,3-diaminopropane (148 mg, 2 mmol) in methanol (5 mL) were added to a pale yellow solution of 3,3′-(3,6-dioxaoctane-1,8-diyldioxy)bis(2-hydroxybenzaldehyde) (780.8 mg, 2 mmol) in methanol (50 mL). This yellow solution was then heated under reflux for 2.5 h and subsequently reduced to dryness.

$La(H_2L_D)Cl_3$: The obtained yellow residue was recrystallised from MeOH/EtOH, filtered off and dried in vacuo. 997 mg, 74% yield. $C_{23}H_{28}Cl_3LaN_2O_6$ (673.73): calcd. C 41.00, H 4.19, N 4.16; found (%) C 40.60, H 4.43, N 3.79. IR: $\tilde{\nu}$ = 1648 cm^{-1} ($\nu_{C=N}$, s). ^1H NMR (300 MHz, CD_3OD, 25 °C): δ = 2.43 (quint, 2 H, $CNCH_2CH_2$), 4.01 (t, 4 H, $CNCH_2$), 4.21 (s, 4 H, CH_2O), 4.37 (t, 4 H, CH_2O), 4.54 (t, 4 H, CH_2O-Ar), 6.73 (t, 2 H, Ar−*H*), 7.18 (dd, 2 H, Ar−*H*), 7.33 (dd, 2 H, Ar−*H*), 8.79 (s, 2 H, *H*C=N). SEM-EDS: La/Cl = 1:3.

$Ce(H_2L_D)Cl_3$: The yellow residue was recrystallised from MeOH/*i*PrOH, filtered off, washed with Et_2O and dried in vacuo. 931 mg, 69% yield. $C_{23}H_{28}CeCl_3N_2O_6$ (674.94): calcd. C 40.93, H 4.18, N 4.15; found C 41.61, H 4.64, N 4.31. IR: $\tilde{\nu}$ = 1639 cm^{-1} ($\nu_{C=N}$, s). ^1H NMR (300 MHz, CD_3OD, 25 °C): δ = 0.56 (s, 4 H, CH_2O), 2.36 (t, 4 H, CH_2O), 3.63 (m, 2 H, $CNCH_2CH_2$), 5.24 (d, 2 H, Ar−*H*), 5.53 (t, 4 H, $CNCH_2$), 6.35 (t, 2 H, Ar−*H*), 7.41 (t, 4 H, CH_2O), 7.94 (d, 2 H, Ar−*H*), 10.57 (s, 2 H, *H*C=N). SEM-EDS: Ce/Cl = 1:3.

$Gd(H_2L_D)Cl_3{\cdot}2H_2O$: The yellow residue was recrystallised from EtOH/*i*PrOH, filtered off, washed with Et_2O and dried in vacuo. 1077 mg, 74% yield. $C_{23}H_{28}Cl_3GdN_2O_6{\cdot}2H_2O$ (728.10): calcd. C 37.94, H 4.43, N 3.85; found C 38.42, H 5.13, N 3.81. IR: $\tilde{\nu}$ = 1653 cm^{-1} ($\nu_{C=N}$, s). SEM-EDS: Gd/Cl = 1:3.

$Tb(H_2L_D)Cl_3{\cdot}7H_2O$: The yellow residue was treated with MeOH/Et_2O and dried in vacuo. 1181 mg, 72% yield. $C_{23}H_{28}Cl_3N_2O_6Tb{\cdot}7H_2O$ (819.84): calcd. C 33.70, H 5.16, N 3.42; found C 33.39, H 4.65, N 3.86. IR: $\tilde{\nu}$ = 1637 cm^{-1} ($\nu_{C=N}$, s). SEM-EDS: Tb/Cl = 1:3.

$NiLn(L_D)Cl_3{\cdot}nH_2O{\cdot}m$EtOH (Ln = La, Ce, Gd, Tb, n = 0−2, m = 0−2): Triethylamine (202 mg, 2 mmol) and $NiCl_2{\cdot}6H_2O$ (237.7 mg, 1 mmol), dissolved in MeOH (2 mL), were added to a yellow solution of $Ln(H_2L_D)Cl_3{\cdot}nH_2O$ (1 mmol) in MeOH/EtOH (for La) or MeOH/*i*PrOH (for Ce,Gd,Tb) (20 mL) that was slightly heated (30 °C). After stirring for 10 min, a pale green precipitate formed. The

suspension was then stirred for a further 20 min and subsequently cooled to room temperature. The resultant pale green powder was collected by filtration, washed with Et_2O and dried in vacuo. Slow diffusion of Et_2O into an EtOH/MeOH solution of the compound produced green crystals. 62% average yield.

$LaNi(L_D)Cl_3$: 464 mg, 63% yield. $C_{23}H_{26}Cl_3LaN_2NiO_6$ (730.42): calcd. C 37.82, H 3.59, N 3.84; found C 37.75, H 4.11, N 3.40 IR: $\tilde{\nu}$ = 1636 cm^{-1} ($\nu_{C=N}$, s). SEM-EDS: Ni/La/Cl = 1:1:3.

$CeNi(L_D)Cl_3$: 461 mg, 63% yield. $C_{23}H_{26}CeCl_3N_2NiO_6$ (731.63): calcd. C 37.76, H 3.58, N 3.83; found C 37.57, H 4.28, N 3.72. IR: $\tilde{\nu}$ = 1634 cm^{-1} ($\nu_{C=N}$, s). SEM-EDS: Ni/Ce/Cl = 1:1:3.

$GdNi(L_B)Cl_3{\cdot}2H_2O{\cdot}EtOH$: 516 mg, 62% yield. $C_{23}H_{26}Cl_3GdN_2NiO_6{\cdot}2H_2O{\cdot}EtOH$ (830.86): calcd. C 36.14, H 4.37, N 3.37; found C 36.50, H 5.08, N 3.45. IR: $\tilde{\nu}$ = 1638 cm^{-1} ($\nu_{C=N}$, s). SEM-EDS: Ni/Gd/Cl = 1:1:3.

$TbNi(L_B)Cl_3{\cdot}2EtOH$: 504 mg, 60% yield. $C_{23}H_{26}Cl_3N_2NiO_6Tb{\cdot}2EtOH$ (842.57): calcd. C 38.49, H 4.55, N 3.32; found C 38.13, H 4.89, N 3.41. IR: $\tilde{\nu}$ = 1628 cm^{-1} ($\nu_{C=N}$, s). SEM-EDS: Ni/Tb/Cl = 1:1:3.

$CuLn(L_D)Cl_3{\cdot}CH_3OH$ (Ln = La, Ce, Gd, Tb): Triethylamine (202 mg, 2 mmol) and $CuCl_2{\cdot}2H_2O$ (170.5 mg, 1 mmol), dissolved in MeOH (2 mL), were added to a yellow solution of $Ln(H_2L_D)Cl_3{\cdot}nH_2O$ (1 mmol) in methanol (for La) or MeOH/EtOH (for Ce,Gd, Tb) (20 mL) that was slightly heated (30 °C). After stirring for 10 min, a green precipitate formed; the suspension was stirred for further 20 min and then cooled to room temperature. The resultant green powder was collected by filtration, washed with Et_2O and dried in vacuo. Slow diffusion of Et_2O into an EtOH/MeOH solution of the compound produced green crystals. 63% average yield.

$LaCu(L_D)Cl_3{\cdot}CH_3OH$: 492 mg, 64% yield. $C_{23}H_{26}Cl_3CuLaN_2O_6{\cdot}CH_3OH$ (767.30): calcd. C 37.57, H 3.94, N 3.60; found C 38.49, H 3.77, N 3.60. IR: $\tilde{\nu}$ = 1625 cm^{-1} ($\nu_{C=N}$, s). SEM-EDS: Cu/La/Cl = 1:1:3.

$CeCu(L_D)Cl_3{\cdot}CH_3OH$: 480 mg, 62% yield. $C_{23}H_{26}CeCl_3CuN_2O_6{\cdot}CH_3OH$ (768.51): calcd. C 37.51, H 3.93, N 3.65; found C 37.84, H 4.02, N 3.87. IR: $\tilde{\nu}$ = 1627 cm^{-1} ($\nu_{C=N}$, s). SEM-EDS: Cu/Ce/Cl = 1:1:3.

$GdCu(L_D)Cl_3{\cdot}CH_3OH$: 495 mg, 63% yield. $C_{23}H_{26}Cl_3CuGdN_2O_6{\cdot}CH_3OH$ (785.64): calcd. C 36.69, H 3.85, N 3.57; found C 37.40, H 3.53, N 3.45. IR: $\tilde{\nu}$ = 1627 cm^{-1} ($\nu_{C=N}$, s). SEM-EDS: Cu/Gd/Cl = 1:1:3.

$TbCu(L_D)Cl_3{\cdot}CH_3OH$: 494 mg, 63% yield. $C_{23}H_{26}N_2O_6TbCuCl_3{\cdot}CH_3OH$ (787.31): calcd. C 36.61, H 3.84, N 3.56; found C 36.82, H 3.94, N 3.74. IR: $\tilde{\nu}$ = 1627 cm^{-1} ($\nu_{C=N}$, s). SEM-EDS: Cu/Tb/Cl = 1:1:3.

$ZnLn(L_D)Cl_3{\cdot}nH_2O{\cdot}mROH$ (Ln = La, Ce, Gd, Tb; n = 0−3; m = 0−1; R = CH_3, CH_3CH_2): Triethylamine (202 mg, 2 mmol) and $ZnCl_2$ (136.28 mg, 1 mmol), dissolved in MeOH (2 mL), were added to a yellow solution of $Ln(H_2L_D)Cl_3{\cdot}nH_2O$ (1 mmol) in methanol or MeOH/EtOH (for La, Gd) (20 mL) that was slightly heated (30 °C). After stirring for 10 min, a pale yellow precipitate formed. The suspension was then stirred for further 20 min and subsequently cooled to room temperature. The obtained pale yellow powder was collected by filtration, washed with Et_2O and dried in vacuo. Slow diffusion of Et_2O into an EtOH/MeOH solution of the compound produced pale yellow crystals. 55% average yield.

$LaZn(L_D)Cl_3{\cdot}CH_3OH$: 439 mg, 57% yield. $C_{23}H_{26}Cl_3LaN_2O_6Zn{\cdot}CH_3OH$ (769.12): calcd. C 37.48, H 3.93, N 3.64; found C 36.86, H 3.49, N 3.53. IR: $\tilde{\nu}$ = 1631 cm^{-1} ($\nu_{C=N}$, s). ^1H NMR (300 MHz, CD_3OD, 25 °C): δ = 2.19 (quint, 2 H, $CNCH_2CH_2$), 4.00 (t, 4 H, $CNCH_2$), 4.20 (s, 4 H, CH_2O), 4.37 (t, 4 H, CH_2O), 4.56 (t, 4 H, CH_2O−Ar), 6.85 (t, 2 H, Ar−*H*), 7.13 (dd, 2 H, Ar−*H*), 7.28 (dd, 2 H, Ar−*H*), 8.41 (s, 2 H, *H*C=N). SEM-EDS: Zn/La/Cl = 1:1:3.

$CeZn(L_D)Cl_3{\cdot}CH_3OH$: 412 mg, 53% yield. $C_{23}H_{26}CeCl_3N_2O_6Zn{\cdot}CH_3OH$ (770.33): calcd. C 37.42, H 3.93, N 3.64; found C 37.42, H 3.68, N 3.66. IR: $\tilde{\nu}$ = 1630 cm^{-1} ($\nu_{C=N}$, s). ^1H NMR (300 MHz, CD_3OD, 25 °C): δ = 0.80 (br. s, 4 H, CH_2O), 1.81 (br. s, 4 H, CH_2O), 2.97 (m, 2 H, $CNCH_2CH_2$), 4.59 (m, 4 H, $CNCH_2$), 5.81 (br. s, 2 H, Ar−*H*), 6.60 (t, 2 H, Ar−*H*), 7.26 (br. s, 4 H, CH_2O), 7.63 (d, 2 H, Ar−*H*), 9.28 (s, 2 H, *H*C=N). SEM-EDS: Zn/Ce/Cl = 1:1:3.

Table 4. Crystal and intensity data for La−Cu, La−Zn and Tb−Cu complexes

Coordinated metals	La−Cu	La−Zn	Tb−Cu
Empirical formula	$C_{24}H_{30}Cl_3CuLaN_2O_7$	$C_{24}H_{30}Cl_3LaN_2O_7Zn$	$C_{24}H_{30}Cl_3CuN_2O_7Tb$
Formula mass	764.30	769.13	787.31
Crystal system	monoclinic	monoclinic	monoclinic
Space group	$P2_1/n$ (No. 14)	$P2_1/n$ (No. 14)	$P2_1/n$ (No. 14)
a [Å]	11.041(2)	11.186(2)	10.967(2)
b [Å]	14.034(3)	14.076(3)	13.851(3)
c [Å]	18.590(4)	18.558(4)	18.625(4)
β [°]	102.74(3)	103.35 (3)	102.68(3)
Cell volume [$Å^3$]	2809(1)	2843(1)	2760(1)
Z	4	4	4
Calcd. density [g/cm^3]	1.814	1.797	1.895
Absorption μ [mm^{-1}] (Mo-K_α)	2.588	2.653	3.648
Range of relative transmission factors [%][a]	91−100	88−100	81−100
θ limits [°]	6.9−56	6.2−56	6.3−56
Data collected/unique	6215/6028	6156/5981	3789/3636
Data observed	5958 [$F \geq 3.5\sigma(F)$]	5878 [$F \geq 3.5\sigma(F)$]	3557 [$F \geq 3.5\sigma(F)$]
No. of parameters (observed per parameter)	320 (18.6)	320 (18.4)	320 (11.1)
R [$\Sigma(\|F_o\| - \|F_c\|)/\Sigma\|F_o\|$]	0.051	0.063	0.067
R_w [$\Sigma w(\|\|F_o\| - \|F_c\|\|)^2/\Sigma w(F_o)^2]^{1/2}$	0.130	0.14	0.15
Highest map residual [$e^-/Å^3$]	1.67	1.22	1.18

[a] Corrections: Lorentz polarization and absorption (empirical, ψ scan).

$GdZn(L_D)Cl_3 \cdot 3H_2O$: 445 mg, 55% yield. $C_{23}H_{26}Cl_3GdN_2O_6Zn \cdot 3H_2O$ (809.46): calcd. C 34.13, H 3.98, N 3.46; found C 33.43, H 3.90, N 3.53. IR: $\tilde{\nu}$ = 1631 cm^{-1} ($\nu_{C=N}$, s). SEM-EDS: Zn/Gd/Cl = 1:1:3.

$TbZn(L_D)Cl_3 \cdot EtOH$: 439 mg, 55% yield. $C_{23}H_{26}Cl_3N_2O_6TbZn \cdot CH_3CH_2OH$ (803.16): calcd. C 37.39, H 4.02, N 3.49; found C 36.82, H 3.80, N 3.51. IR: $\tilde{\nu}$ = 1632 cm^{-1} ($\nu_{C=N}$, s). SEM-EDS: Zn/Tb/Cl = 1:1:3.

X-ray Crystallography: Diffraction data were collected at room temperature with a Philips PW1100 automatic four-circle diffractometer (FEBO System) using graphite-monochromated Mo-K_α radiation and the ω-2θ scan mode. Lattice parameters were obtained from least-squares refinement of the setting angles of 25 reflections with $10° \leq 2\theta \leq 24°$. Table 4 summarises the crystallographic data and structure refinement. No sign of crystal deterioration was revealed by monitoring three standard reflections after every 200 measurements. Structures were solved by standard Patterson methods and subsequently completed by a combination of least-squares techniques and Fourier syntheses with the SHELX program.[54] All benzene rings were refined as rigid bodies, hydrogen atoms were included in idealised positions with fixed C−H distances (0.97Å) and isotropic temperature factors fixed to 1.2 times U(eq) of the respective carbon atom. Selected bond lengths and angles pertinent to the coordination spheres are given in Tables 1 and 2 and representative torsion angles in Table 3. Additional crystallographic data, atomic coordinates, anisotropic thermal parameters, and full listings of bond lengths and angles are provided as supplementary material. CCDC-244706, -244707 and -244708 contain the supplementary crystallographic data for this paper. These data can be obtained free of charge at www.ccdc.cam.ac.uk/conts/retrieving.html [or from the Cambridge Crystallographic Data Centre, 12 Union Road, Cambridge CB2 1EZ, UK; Fax: (internat.) + 44-1223-336-033; E-mail: deposit@ccdc.cam.ac.uk]. Final geometrical calculations and drawings were carried out with the PARST program[55] and the XP utility of the Siemens package,[56] respectively, running on a DIGITAL ALPHA-AXP 300 computer. X-ray powder diffraction measurements were carried out with a Philips X'Pert diffractometer (40 kV, 35 mA) using graphite-monochromated Cu-K_α radiation in the range $5° < 2\theta < 80°$. The simulated powder diffraction pattern was obtained by means of the SHELXTL program (Bruker ASX, 1998) using the single-crystal diffraction data of the La−Cu complex.

Acknowledgments

We thank Mr. A. Aguiari, Mr. E. Bullita and Mrs. A. Moresco for their technical assistance. We also thank MIUR project FIRB-RBNE019H9 K for financial support. A. C. and L. S. thank FIRB RBNE01YLKN and CNR, Italy.

[1] P. A. Vigato, S. Tamburini, *Coord. Chem. Rev.*, in press.
[2] [2a] N. F. Curtis, *Coord. Chem. Rev.* **1968**, *3*, 3. [2b] D. H. Busch, *Science* **1971**, *171*, 241. [2c] S. M. Nelson, *Pure Appl. Chem.* **1980**, *52*, 2461.
[3] V. Alexander, *Chem. Rev.* **1995**, *95*, 273.
[4] [4a] D. E. Fenton, H. Okawa, *Chem. Ber./Recueil* **1997**, *130*, 433. [4b] S. R. Collinson, D. E. Fenton, *Coord. Chem. Rev.* **1996**, *148*, 19. [4c] D. E. Fenton, *Pure Appl. Chem.* **1986**, *58*, 1437.
[5] [5a] L. F. Lindoy, *The Chemistry of Macrocyclic Ligand Complexes*, Cambridge University, Cambridge, U. K., **1989**. [5b] L. F. Lindoy, *Pure Appl. Chem.* **1989**, *61*, 1575. [5c] L. F. Lindoy *Synthesis of Macrocycle: The Design of Selective Complexing Agents* (Eds: R. M. Izatt, J. J. Christensen), Wiley, New York, **1987**, p. 53.
[6] P. Guerriero, S. Tamburini, P. A. Vigato, *Coord. Chem. Rev.* **1995**, *139*, 17.
[7] O. Kahn, *Advances in Inorganic Chemistry* (Ed.: A. G. Sykes), Academic Press, S. Diego (USA), **1995**, vol. 43, p. 179.
[8] K. S. Murray, *Advances in Inorganic Chemistry* (Ed.: A. G. Sykes), Academic Press, S. Diego (USA), **1995**, vol. 43, p. 261.
[9] [9a] *Crown Compounds: Toward Future Applications* (Ed.: S. R. Coper), VCH Publishers Inc., New York, **1992**. [9b] *Coordination Chemistry of Macrocyclic Compounds* (Ed.: G. A. Melson), Plenium Press, New York, **1979**. [9c] A. Martell, J. Penitka, D. Kong, *Coord. Chem. Rev.* **2001**, *55*, 216−217.
[10] P. A. Vigato, P. Guerriero, S. Tamburini, R. Seraglia, P. Traldi, *Org. Mass Spectrom.* **1990**, *25*, 420.
[11] P. Guerriero, S. Tamburini, P. A. Vigato, R. Seraglia, P. Traldi, *Org. Mass Spectrom.* **1992**, *27*, 231.
[12] P. Guerriero, S. Tamburini, P. A. Vigato, S. Catinella, P. Traldi, *Rapid Commun. Mass Spectrom.* **1992**, *6*, 741.
[13] S. Catinella, P. Traldi, P. Guerriero, S. Tamburini, P. A. Vigato, *Rapid Commun. Mass Spectrom.* **1994**, *8*, 111.
[14] M. Coppola, S. Catinella, P. Traldi, P. Guerriero, S. Tamburini, P. A. Vigato, *Org. Mass Spectrom.* **1994**, *29*, 566.
[15] P. Tomasin, S. Tamburini, P. A. Vigato, M. D'Alpaos, P. Traldi, *Rapid Commun. Mass Spectrom.* **1997**, *11*, 494.
[16] M. D'Alpaos, S. Tamburini, P. Tomasin, P. A. Vigato, P. Traldi, *Rapid Commun. Mass Spectrom.* **1997**, *11*, 1909.
[17] P. A. Vigato, S. Tamburini, D. E. Fenton, *Coord. Chem. Rev.* **1990**, *106*, 25.
[18] D. E. Fenton, P. A. Vigato, *Chem. Soc. Rev.* **1988**, *17*, 89.
[19] H. Okawa, H. Furutachi, D. E. Fenton, *Coord. Chem. Rev.* **1998**, *174*, 51.
[20] V. Amendola, C. Brusoni, L. Fabbrizzi, C. Mangano, H. Miller, P. Pallavicini, A. Pernotti, A. Taglietti, *J. Chem. Soc., Dalton Trans.* **2001**, 3528.
[21] [21a] V. Amendola, L. Fabbrizzi, L. Granelli, C. Maggi, C. Mangano, P. Pallavicini, M. Zema, *Inorg. Chem.* **2001**, *40*, 3579. [21b] V. Amendola, L. Fabbrizzi, P. Pallavicini, E. Sartirana, A. Taglietti, *Inorg. Chem.* **2003**, *42*, 1632.
[22] L. Fabbrizzi, F. Foti, P. Pallavicini, S. Patroni, A. Taglietti, *Atti del VI Congresso Nazionale di Chimica Supramolecolare*, Urbino, **2003**, P62, p. 201.
[23] M. Botta, U. Casellato, C. Scalco, S. Tamburini, P. Tomasin, P. A. Vigato, S. Aime, *Chem. Eur. J.* **2002**, *8*, 3917.
[24] N. Brianese, U. Casellato, S. Tamburini, P. Tomasin, P. A. Vigato, *Inorg. Chem. Commun.* **1999**, *2*, 149.
[25] U. Casellato, S. Tamburini, P. Tomasin, P. A. Vigato, S. Aime, A. Barge, M. Botta, *Chem. Commun.* **2000**, 145.
[26] A. D. Sherry, C. F. G. C. Geraldes in *Lanthanide Probes in Life, Chemical and Earth Sciences* (Eds.: J.-C. G. Bunzli, G. R. Choppin), Elsevier, Amsterdam, **1989**, chapter 4.
[27] [27a] R. B. Hutchinson, J. I. Shapiro, *Concepts Magn. Reson.* **1991**, *3*, 215. [27b] C. S. Springer, Jr., in *NMR Techniques in the Study of Cardiovascular Structure and Function* (Eds.: M. Osbakken, J. Haselgrove), Futura Publishing, New York, **1988**, chapter 4.
[28] A. Barge, M. Botta, S. Tamburini, P. A. Vigato, *VI Congresso Nazionale di Chimica Supramolecolare*, Urbino, September 7−10, **2003**, P64, p.205.
[29] C. J. Van Staveren, J. Van Erden, F. C. J. M. Van Veggel, S. Harkema, D. Reinhoudt, *J. Am. Chem. Soc.* **1988**, *110*, 4994.
[30] [30a] F. C. J. M. Van Veggel, M. Bos, S. Harkema, W. Verboom, D. N. Reinhoudt, *Angew. Chem. Int. Ed. Engl.* **1989**, *28*, 749. [30b] F. C. J. M. Van Veggel, M. Bos, S. Harkema, H. Van Bovenkamp, W. Verboom, J. Reedijk, D. N. Reinhoudt, *J. Org. Chem.* **1991**, *56*, 22.
[31] N. Brianese, U. Casellato, S. Tamburini, P. Tomasin, P. A. Vigato, *Inorg. Chim. Acta* **1999**, *293*, 178.
[32] P. Di Bernardo, P. Zanonato, personal communication.
[33] [33a] J.-P. Costes, F. Dahan, F. Nicodeme, *Inorg. Chem.* **2003**, *42*, 6556. [33b] W. Xie, M. J. Heeg, P. G. Wang, *Inorg. Chem.* **1999**, *38*, 2541. [33c] K. Binnemans, Y. G. Galyametdinov, R.

Van Deun, D. W. Bruce, S. R. Collinson, A. P. Polishchuk, I. Bikchantaev, W. Haase, A. V. Prosvirin, L. Tinchurina, I. Litvinov, A. Gubajdullin, A. Rakhmatullin, K. Uytterhoeven, L. Van Meervelt, *J. Am. Chem. Soc.* **2000**, *122*, 4335.
[34] C. Benelli, D. Gatteschi, *Chem. Rev.* **2002**, *102*, 2369 and references cited therein.
[35] A. Bencini, A. Benelli, A. Caneschi, R. L. Carlin, A. Dei, D. Gatteschi, *J. Am. Chem. Soc.* **1985**, *107*, 8128.
[36] M. Andruh, I. Ramade, E. Codjovi, O. Guillou, O. Kahn, J. C. Trombe, *J. Am. Chem. Soc.* **1993**, *115*, 1822.
[37] J. P. Costes, F. Dahan, A. Dupuis, J. P. Laurent, *Inorg. Chem.* **1996**, *35*, 2400.
[38] J.-P. Sutter, M. L. Kahn, S. Golhen, L. Ouahab, O. Kahn, *Chem. Eur. J.* **1998**, *4*, 571.
[39] J. P. Costes, F. Dahan, A. Dupuis, J. P. Laurent, *Inorg. Chem.* **2000**, *39*, 169.
[40] Y. Kobayashi, S. Ueki, T. Ishida, T. Nogami, *Chem. Phys. Lett.* **2003**, *378*, 337.
[41] A. Bencini., D. Gatteschi in *Transition Metal Chemistry* (Eds.: B. N. Figgis, G. Melson) Marcel Dekker, New York, **1982**, vol. 8, p. 1.
[42] C. J. H. Jacobsen, E. Pedersen, J. Villadsen, H. Weihe, *Inorg. Chem.* **1993**, *32*, 1216.
[43] O. Kahn, *Molecular Magnetism*, VCH, New York, **1993**.
[44] C. J. O'Connor, *Prog. Inorg. Chem.* **1982**, *29*, 103.
[45] J. P. Costes, F. Dahan, A. Dupuis, J. P. Laurent, *Chem. Eur. J.* **1998**, *4*, 1616.
[46] M. L. Kahn, C. Mathoniere, O. Kahn, *Inorg. Chem.* **1999**, *38*, 3692.
[47] M. L. Kahn, J. P. Sutter, S. Golhen, P. Guionneau, L. Ouahab, O. Kahn, D. Chasseau, *J. Am. Chem. Soc.* **2000**, *122*, 3413.
[48] J. P. Sutter, M. L. Kahn, O. Kahn, *Adv. Mater.* **1999**, *11*, 863.
[49] A. Figuerola, C. Diaz, J. Ribas, V. Tangoulis, J. Granell, F. Lloret, J. Mahia, M. Maestro, *Inorg. Chem.* **2003**, *42*, 641.
[50] A. Caneschi, A. Dei, D. Gatteschi, S. Poussereau, L. Sorace, *Dalton Trans.*, submitted for publication.
[51] R. D. L. Carlin, *Magnetochemistry*, Springer Verlag, Berlin, **1986**.
[52] A. Caneschi, A. Dei, D. Gatteschi, C. A. Massa, L. A. Pardi, S. Poussereau, L. Sorace, *Chem. Phys. Lett.* **2003**, *371*, 694.
[53] D. D. Perrin, W. L. Armarego, D. R. Perrin, *Purification of Laboratory Chemicals*, 2nd ed., Pergamon Press, Oxford, **1982**, p. 229.
[54] G. M. Sheldrick, C. Kruger, R. Goddard (Eds.), *SHELX-86, Crystallographic Computing 3*, Oxford University Press, London, **1985**, p. 175; G. M. Sheldrick, *SHELXL-93, Program for Crystal Structure Refinement*, University of Göttingen, Germany, **1993**.
[55] M. Nardelli, *J. Appl. Crystallogr.* **1995**, *28*, 659.
[56] G. M. Sheldrick, *SHELXTL-PLUS*, version 4.2, Siemens Analytical X-ray Instruments Inc., Madison, WI, **1991**.
[57] [57a] P. P. Morgan, J. M. Beynon, R. M. Bateman, B. M. Green, *Int. J. Mass Spectrom. Ion Phys.* **1978**, *28*, 171. [57b] M. Barber, R. S. Bordoli, R. D. Sedgwick, A. M. Taylor, *Chem. Commun.* **1981**, *7*, 1716.

Received February 17, 2004
Early View Article
Published Online August 3, 2004

